Available online at www.sciencedirect.com
ScienceDirect
Scripta Materialia xxx (2010) xxx–xxx
Scripta MATERIALIA
www.elsevier.com/locate/scriptamat

Coupling quantum and continuum scales to predict crack tip dislocation nucleation

A.K. Nair,[a] D.H. Warner,[a,*] R.G. Hennig[b] and W.A. Curtin[c]

[a]*School of Civil and Environmental Engineering, Cornell University, Ithaca, NY 14853, USA*
[b]*Department of Materials Science and Engineering, Cornell University, Ithaca, NY 14853, USA*
[c]*Division of Engineering, Brown University, Providence, RI 02912, USA*

Received 2 July 2010; revised 19 August 2010; accepted 19 August 2010

A quantum-continuum multiscale coupling of Kohn–Sham density functional theory to continuum material is presented that can handle mechanics problems in metals when long-range stress fields are present, such as occurs for dislocations and cracks. The method has quantifiable and controllable coupling errors that can be minimized at computationally tractable system sizes. Using both generalized gradient and local density approximation exchange–correlation functionals, the nucleation of a dislocation from a crack tip in aluminum is then predicted. Both functionals yield similar results, and predictions using Rice's continuum Peierls model are within 20% of the quantum values. This multiscale method is easily extendable to crack-tip problems involving alloys and chemical embrittlements.

Keywords: Multiscale modeling; Density functional theory; Fracture; Metal and alloys; Dislocations

Increasing accessibility to large computational resources along with the continued refinement of Kohn–Sham density functional theory (KSDFT) has led to a succession of insightful quantum mechanical calculations. However, despite these advances, applications requiring the relaxation of long-range elastic fields remain difficult. Crack tip behavior is a quintessential example of this difficulty, with a long-range elastic field while phenomena are controlled by local crack tip bond breaking. Modeling cracks thus requires a concurrent multiscale approach if powerful quantum mechanical methods such as KSDFT are to be utilized at the crack tip. Embedding a small region of atoms governed by quantum mechanics within a larger region governed by classical mechanics makes computational expenses tractable while capturing the long-range strain field [1]. Prior investigations involving crack tips have been limited to covalently bonded materials, e.g. Si, where the locality of the bonding underlies the accuracy of the multiscale coupling method [2–5]. While some elegant KSDFT multiscale strategies have been developed for metals, applications have been limited to dislocations and point defects in infinite crystals [6,7].

In this letter we present a multiscale method that couples a region governed by quantum mechanics to a surrounding region governed by a continuum material description. The underlying theory builds on the multiscale coupled atomistic discrete dislocation (CADD) model [8], with the atomistic region of CADD replaced by a quantum–mechanical region. We thus label the method as QM-CADD. The method is versatile and general, being able to use any computationally tractable quantum mechanics methodology, and applicable to non-metals as well as metals. The quantum-continuum coupling strategy is straightforward and easy to implement, but most importantly the method has quantifiable and controllable coupling errors.

Here, we validate the accuracy of the coupling method with several test problems and then use the model to predict nucleation of a dislocation from a crack tip in aluminum, a problem with a rich history [9–11], thus simultaneously demonstrating success in studying (i) a challenging material system, due to the long-range electronic effects associated with a large Fermi wave vector; (ii) a complex boundary value problem; and (iii) an important mechanical phenomenon simultaneously involving bond breaking, new surface and defect creation.

The QM-CADD coupling method involves the solution of two distinct problems, one in the quantum

* Corresponding author. Tel.: +1 607 255 7155; e-mail: dhw52@cornell.edu

1359-6462/$ - see front matter © 2010 Acta Materialia Inc. Published by Elsevier Ltd. All rights reserved.
doi:10.1016/j.scriptamat.2010.08.038

domain and one in the continuum domain, that are coupled through self-consistent boundary conditions [10]. A schematic, within the context of the dislocation nucleation problem studied here, is shown in Figure 1. Figure 1b displays four distinct regions: an inner region (gray ions); an interface (black ions); an outer "pad" region (white ions); and a continuum region (finite element method (FEM) mesh). The continuum region extends into the interface ions, which serve as boundary nodes of the FEM mesh. The "pad" ions overlap with the continuum region, and their displacements from the perfect crystal positions are obtained by interpolation of the FEM displacement fields to the reference crystal pad ion positions. The inner and interface ion positions are obtained from a quantum mechanical calculation. The quantum mechanical cell consists of a periodic cell containing the inner, interface and pad ions, and associated electron density, surrounded by a vacuum region, as shown in Figure 1c. For a given applied loading on the outer boundaries of the problem, a single iteration of the solution procedure consists of the following algorithm: (i) the positions of the ions in the atomistic, interface and pad regions are given as input to a quantum mechanics simulation for the computation of the electronic ground state; (ii) the positions of the ions in the inner and interface regions are then updated using the quantum-derived Hellmann–Feynmann forces; (iii) the new interface ion positions are used as a displacement boundary condition for the continuum region, with the finite element method determining the continuum displacement field; (iv) the continuum displacement fields are then used to determine new positions of the pad ions, completing the iteration.

The non-local nature of quantum-mechanics-based interatomic forces, which depend on the charge density over the entire quantum mechanical cell, is a challenge for any multiscale method. Truncation of the QM domain generates spurious long-range forces associated with Friedel oscillations in the electron density, which is particularly problematic in metals. However, in practice the influence of the charge density on the force of a particular ion decays with distance, even in metals [2]. To control such spurious forces on the inner and interface ions, QM-CADD uses the pad ions to isolate the inner domain from the electronic surface in the quantum mechanical cell. The pad ion positions, being determined by the continuum FEM solution, are in the correct positions for the posed boundary value problem so that the spurious forces are only due to electronic effects. A pad region of sufficient thickness can thus minimize these spurious forces. Determination of a suitable thickness is problem- and material-dependent, and represents a balance between accuracy and computational cost. The QM-CADD method has no spurious "ghost forces" at the interface because the interface is mainly a kinematic constraint and forces in the quantum region are computed solely from a quantum calculation.

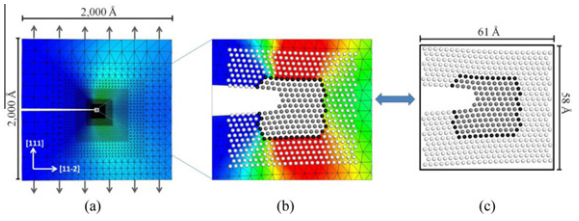

Figure 1. Schematic of the computational model and geometry for studying crack tip dislocation nucleation; (a) overall geometry with color contours showing uniaxial strain in the vertical direction; (b) close-up view of the near tip region, showing the inner ions (gray), the interface ions (black) and the pad ions (white); (c) quantum simulation cell consisting of inner, interface and pad ions surrounded by vacuum in a periodic unit cell. The three-dimensional atomic lattice is projected onto the two-dimensional plane for visualization.

In addition to the use of a pad region in the quantum–mechanical cell, the other main approximation in the QM-CADD is in the representation of the continuum region material properties, starting at the interface. At a minimum, the lattice constant and elastic constants in the continuum region are made identical to those corresponding to the quantum-computed properties of the material, which is computationally most efficient. The use of linear elasticity limits deformation to small strains so that the size of the inner atomistic domain must be chosen to encompass the nonlinear elastic region while balancing the computational expense associated with a larger atomistic domain. The continuum material response can be enhanced by using either nonlinear elasticity or by invoking the Cauchy–Born rule to obtain the material response directly from quantum–mechanical calculations on periodic deformed unit cells, as in the quasicontinuum method [12]. Below we demonstrate the linear elasticity is sufficiently accurate for the domain sizes used.

When the continuum region is modeled as linearly elastic, this coupling method can be considered an extension of the lattice Green function (LGF) approach proposed by Woodward and Rao [13] with the LGFs replaced by a numerical finite element solution of the continuum deformation. The structure of both CADD and LGF methods circumvents, by construction, the challenges associated with so-called "ghost forces" at the coupling interface that often arise [7,12]. Modeling the continuum domain using the finite element framework allows for the study of arbitrary geometries with free surfaces, such as a crack tip. Also, when the continuum domain is linear elastic, the QM-CADD method can include discrete dislocation plasticity in the continuum domain exactly as done in CADD [14].

In this work, we use the plane-wave KSDFT code VASP [15] to compute forces in the quantum mechanical cell. The simulations are performed with both the local density (LDA) and generalized gradient (GGA) approximations. The 1*s*, 2*s* and 2*p* core electrons of Al are described by an ultrasoft pseudopotential [16]. A kinetic energy cutoff of 192 eV was used with a $1 \times 1 \times 8$ *k*-point mesh and a Methfessel–Paxton smearing of 1 eV. The dimensions of the periodic KSDFT simulation cell are chosen so that lattice periodicity was maintained in the out of plane dimension while the in-plane dimensions are chosen to be 3 Å larger than the most protruding atoms (Fig. 1c). This distance is chosen to minimize the amount of vacuum in the cell yet restrict atoms from becoming too close to one another. The continuum region is modeled as an anisotropic linear elastic material with lattice and elastic constants chosen to match those of the quantum material [6]. For each iteration, ions in the inner and interface regions are moved by one conjugate

Please cite this article in press as: A.K. Nair et al., Scripta Mater. (2010), doi:10.1016/j.scriptamat.2010.08.038

gradient step while the out-of-balance forces in the continuum region are completely eliminated by using the inverted finite element stiffness matrix. When all out-of-balance forces in the inner region were below 8 meV Å^{-1}, the system is considered to be in mechanical equilibrium.

The QM-CADD implementation is validated, and the required inner and pad region sizes determined, in two ways. First, a perfect crystal under zero applied load is studied for a 55 × 50 Å quantum cell with a pad thickness of 13 Å, and a total of 452 ions with 119 ions in the inner and interface regions. Forces on the ions in the inner region are then computed. For the KSDFT parameters and crystallographic surfaces used in this study, the 13 Å pad is sufficient to achieve forces of less than the 8 meV Å^{-1} tolerance throughout the inner domain. Forces just outside the interface ions are 11 meV Å^{-1}, demonstrating the forces that would be generated by using a thinner pad. The perfect crystal test is an easy test for establishing an adequate pad region for any material choice. Second, using the quantum cell and pad thickness, the method was used to compute the core structure of a screw dislocation core in Al. The Nye tensor [17] distribution of the dislocation burgers vector of our converged core is in excellent agreement with the result of LGF results of Woodward et al. using the same GGA KSDFT parameters [6], and showing a dissociation distance of 5 Å. Since the screw dislocation has a long-range ($1/r$) stress field, these two results taken together show that, for Al, the inner and pad regions are both large enough such that the effects of both linear elasticity and the vacuum interface are sufficiently small.

As a first application, we investigate dislocation nucleation from a crack on a (1 1 1) plane with a $[\bar{1}\,1\,0]$ crack front in fcc Al. The crack is created by removing three planes of atoms over half of the total simulation domain of dimensions 200 × 200 nm (Fig. 1a). The quantum cell is similar to those studied above, containing 486 ions in a 61 × 58 Å box with a pad thickness of 13 Å surrounding a 31 × 28 Å region containing 136 ions (Fig. 1c). A remote loading corresponding to the stress intensity K_I for the linear elastic anisotropic mode I displacement field of a sharp crack is applied, starting from an initial value near that predicted by the Rice nucleation criteria [11]. At fixed K_I, mechanical equilibrium in the system is achieved after approximately 60 force calculations. For the most computationally demanding GGA simulations, each force calculation requires approximately two hours on 512 processors. The boundary displacement field is then incremented by $\Delta K_I = 0.015$ eV Å$^{-2.5}$ or less and the system again relaxed to equilibrium. Loading is stopped when dislocation nucleation is observed, yielding a value for the critical stress intensity, K_{In}, for dislocation nucleation.

In the crack problem, free surfaces cross the quantum/continuum interface, so the true surface response of the quantum material must be accurately represented in the pad region. The most crucial component is the surface relaxation, i.e. the unstressed positions of the ions on the surface, which differ relative to the bulk equilibrium lattice positions. Independent KSDFT simulations on (1 1 1) Al surfaces yield displacements normal to the surface of −0.0287 and −0.0323 Å for LDA and GGA, respectively, with negative values corresponding to outward surface relaxation, consistent with experiments on Al [18]. These displacements are imposed on the surface ions in the pad, while higher-order effects, such as the relaxation of next-nearest surface planes and altered elastic constants near the surface, are not considered.

For reference and comparison, we also study the nucleation problem within the framework of embedded atom method (EAM) potentials, using the Ercolessi–Adams and Mishin–Farkas potentials [19,20]. For these systems, the surface relaxations are −0.0175 and 0.007 Å, respectively. We also use the Ercolessi–Adams EAM system to study the dependence of the crack tip emission point K_{In} as a function of the size of the atomistic region to probe the effect of non-linearity. For the same size as used in the quantum cell, K_{In} is overestimated by 5% relative to much larger size, which we consider an acceptable error.

At the measured K_{In}, mechanical relaxation of the ion positions near the crack tip involves a significant shearing in the $[1\,1\,\bar{2}]$ direction on the (1 1 1) plane consistent with the nucleation and subsequent glide of a pure edge partial dislocation away from the crack tip (Fig. 2). The emerging dislocation core can be seen by both a disregistry in the atomic lattice and a redistribution of electronic charge.

Table 1 shows the stress intensity K_{In} at which nucleation occurs for the GGA and LDA KSDFT approximations. The two results are quite similar. To interpret these results, we consider Rice's crack tip dislocation nucleation criterion, based on a Peierls slip model along the slip plane at the crack tip [11]. For the crack geometry and crystallography used here, that model predicts nucleation at

$$K_{in}^{Rice} = 2.60\sqrt{2\gamma_{us}\mu^*} \tag{1}$$

where γ_{us} is the unstable stacking fault energy and μ^* is the effective shear modulus along the plane of emission,

$$\mu^* = \frac{(C_{11} - C_{12} + C_{44})}{3(1 - (C_{11} + 4C_{12} - 2C_{44})/(4C_{11} + 6C_{12}2C_{44}))} \tag{2}$$

Table 1 shows the values of γ_{us} and μ^* computed within the GGA and LDA KSDFT methods, and the resulting predictions for K_{In}. The agreement is generally good, although the Rice model predicts a greater differ-

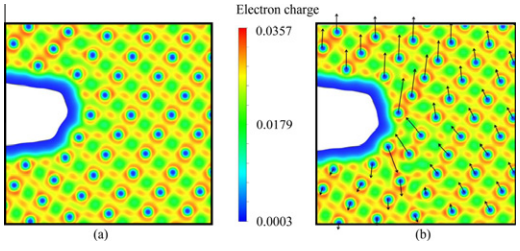

Figure 2. Charge density contours on the $(1\,\bar{1}\,0)$ plane near the crack tip for the GGA KSDFT simulation plotted using VESTA [24]; (a) equilibrium configuration at the load step immediately before nucleation, $K_I = 0.215$ eV Å$^{-2.5}$; (b) non-equilibrium configuration during dislocation nucleation at a load of $K_I = 0.230$ eV Å$^{-2.5}$. The vectors are proportional to the displacements of ions relative to their equilibrium positions in (a).

Please cite this article in press as: A.K. Nair et al., Scripta Mater. (2010), doi:10.1016/j.scriptamat.2010.08.038

Table 1. Stress intensity factor K_{In} for crack tip dislocation nucleation as predicted by LDA and GGA KSDFT methods and by empirical EAM potentials, together with the (1 1 1) surface stresses and the predictions of K_{In} by the Rice theory using the unstable stacking fault energy and effective shear modulus from each material model (1.60 eV Å$^{-2.5}$ = 1.00 MPa m$^{1/2}$).

	LDA-DFT	GGA-DFT	Ercolessi–Adams	Mishin–Farkas
Simulated K_{In} (eV Å$^{-2.5}$)	0.245	0.230	0.226	0.182
Rice criterion K_{In} (eV Å$^{-2.5}$)	0.227	0.181	0.174	0.188
Unstable stacking fault energy γ_{us} (eV Å^{-2})	0.013	0.0095	0.0078	0.0101
Anisotropic elastic constant μ^* (GPa)	46.9	40.8	44.9	42.1
(1 1 1) surface stress (eV Å^{-2})	0.071	0.065	0.057	0.057

ence than found in the quantum results. A discrepancy between the direct simulations and Rice's model is often attributed to the influence of surface stresses [9]. However, for the material models studied here the magnitude of surface stress does not correlate with the magnitude of the discrepancy across models (Table 1). Additional potential sources for the discrepancy between Rice's model and the direct simulations are the pressure dependence of γ_{us} [12,23], the surface ledge creation energy [21] and differences in crack tip geometry (theoretically sharp vs. blunted) [22]. KSDFT LDA is known to over-predict elastic constants and stacking fault energies, but predicts nearly the same K_{In} value as obtained by the GGA simulation. Thus, the high coincidence of K_{In} values from the LDA and GGA approaches is most likely due to a cancellation of competing factors. The physically reasonable partial dislocation emission and its occurrence at applied stress intensity comparable to an established (but not exact) theory generally demonstrates the success of our multiscale quantum-mechanics-based framework for handling complex boundary value problems in metals.

Table 1 also shows results obtained for the two EAM potentials. The Ercolessi-Adams potential yields a K_{In} value comparable to the two quantum-derived values, while the Mishin–Farkas potential yields a rather lower value. The corresponding predictions of the Rice model are also shown, with good agreement found for the Mishin–Farkas potential but a larger discrepancy for the Ercolessi–Adams potential. Interestingly, the Mishin–Farkas potential was carefully designed to match KSDFT GGA material properties thought to be important in deformation processes, such as the elastic constants and γ_{us}, yet its K_{In} value is significantly lower than that obtained by direct simulations using GGA. Conversely, the Ercolessi–Adams potential substantially under predicts the unstable stacking fault energy but yields a K_{In} value much closer to the KSDFT results. Overall, while differences in K_{In} are present, they are not exceptionally large. This reinforces the usefulness of Al EAM potentials for reasonably quantitative predictions but also demonstrates that even some of the best EAM potentials differ by 20% relative to a quantum-mechanics-based analysis.

We have presented a general framework for quantum-continuum multiscale coupling that is easily implemented and can address complex geometries and loadings in metallic materials. The method contains two quantifiable and controllable sources of error originating from the non-local nature of the quantum ionic forces and the range of applicability of continuum elasticity. The method has been validated in several ways, and then used to predict the critical stress intensity factor for dislocation nucleation from a crack tip in Al using KSDFT. Despite differences in material constants, the LDA and GGA approaches yield similar values that are in reasonable agreement with Rice's model. EAM potentials yield values in reasonable agreement with the quantum predictions. With the method and application to crack tip phenomena now established, the foundation is set for future studies using KSDFT to predict the effects of chemistry at the crack tip on both crack growth and dislocation emission.

D.H.W. acknowledges support from Paul Hess at ONR (Grant N00014-08-1-0862 and N00014-10-1-0323) and Ed Glaessgen and Steve Smith at NASA (Grant NNX08BA39A). W.A.C. acknowledges support from NASA Langley Research Center (Grant NNX07AU56A) and the NSF through the MRSEC on "Micro- and Nanomechanics of Materials" at Brown University (DMR-0520651).

[1] N. Bernstein, J.R. Kermode, G. Csanyi, Rep. Prog. Phys. 72 (2) (2009) 026501.
[2] S. Ismail-Beigi, T.A. Arias, Phys. Rev. Lett. 82 (10) (1999) 1227.
[3] J.Q. Broughton et al., Phys. Rev. B 60 (4) (1999) 2391.
[4] S. Ogata et al., J. Appl. Phys. 95 (10) (2004) 5316.
[5] J.R. Kermode et al., Nature 455 (7217) (2008) 1224.
[6] C. Woodward et al., Phys. Rev. Lett. 100 (4) (2008) 4.
[7] G. Lu, E.B. Tadmor, E. Kaxiras, Phys. Rev. B 73 (2) (2006) 024108.
[8] L.E. Shilkrot, R.E. Miller, W.A. Curtin, Phys. Rev. Lett. 89 (2) (2002) 025501.
[9] J. Knap, K. Sieradzki, Phys. Rev. Lett. 82 (8) (1999) 1700.
[10] Y. Sun, G.E. Beltz, J.R. Rice, Mater. Sci. Eng. A A170 (1–2) (1993) 67.
[11] J.R. Rice, J. Mech. Phys. Solids 40 (2) (1992) 239.
[12] V.B. Shenoy et al., J. Mech. Phys. Solids 47 (3) (1999) 611.
[13] C. Woodward, S.I. Rao, Phys. Rev. Lett. 88 (21) (2002) 216402.
[14] E. van der Giessen, A. Needleman, Modell. Simul. Mater. Sci. Eng. 3 (5) (1995) 689.
[15] G. Kresse, J. Hafner, Phys. Rev. B 48 (17) (1993) 13115.
[16] G. Kresse, J. Hafner, J. Phys. Cond. Mat. 6 (40) (1994) 8245.
[17] C.S. Hartley, Y. Mishin, Acta Mater. 53 (5) (2005) 1313.
[18] J. Wan et al., Modelling Simul. Mater. Sci. Eng. 7 (2) (1999) 189.
[19] F. Ercolessi, J.B. Adams, Europhysics Lett. 26 (8) (1994) 583.
[20] Y. Mishin et al., Phys. Rev. B 59 (5) (1999) 3393.
[21] G. Schoeck, Mater. Sci. Eng. A-Struct. Mater. Prop. Microstruct. Process. 356 (1–2) (2003) 93.
[22] L.L. Fischer, G.E. Beltz, J. Mech. Phys. Solids 49 (2001) 635.
[23] C. Brandl, P.M. Derlet, H. Van Swygenhoven, Phys. Rev. B 76 (5) (2007) 054124.
[24] K. Momma, F. Izumi, J. Appl. Cryst. 41 (3) (2008) 653.